Supporting Information

Operando X-Ray Mapping of Ion Transport and Arrangement in a Carbon-Based Supercapacitor Electrode

Malina Seyffertitz[1,2#], Max Valentin Rauscher[1], Sebastian Stock[1], Sylvio Haas[3], Peter Moharitsch[1], Oskar Paris[1*]

1 Chair of Physics, Montanuniversitaet Leoben, AUSTRIA

2 Yusuf Hamied Department of Chemistry, University of Cambridge, UNITED KINGDOM

3 Deutsches Elektronen Synchrotron DESY, GERMANY

Corresponding authors: #ms3216@cam.ac.uk, *oskar.paris@unileoben.ac.at

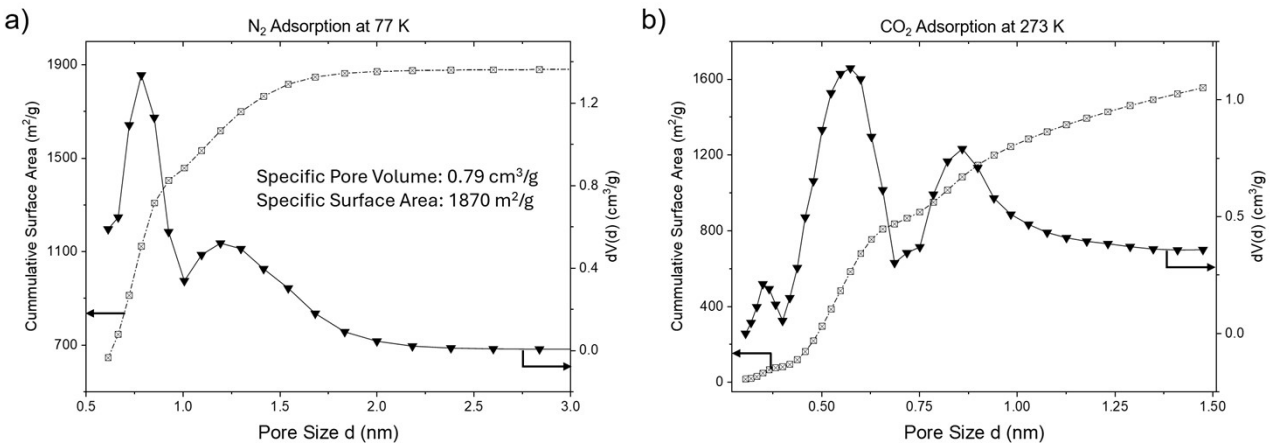

SI Figure S1: ***Pore size distribution of the activated carbon electrode****. Cumulative surface area (open squares, left axis) and pore size distribution (filled triangles, right axis) of the MSP-20X activated carbon electrode with 5 wt.% PTFE binder, derived from a) nitrogen gas adsorption isotherms at 77K using a carbon slit-pore QSDFT equilibrium model and b) carbon dioxide gas adsorption isotherms at 273 K and a NLDFT model.*

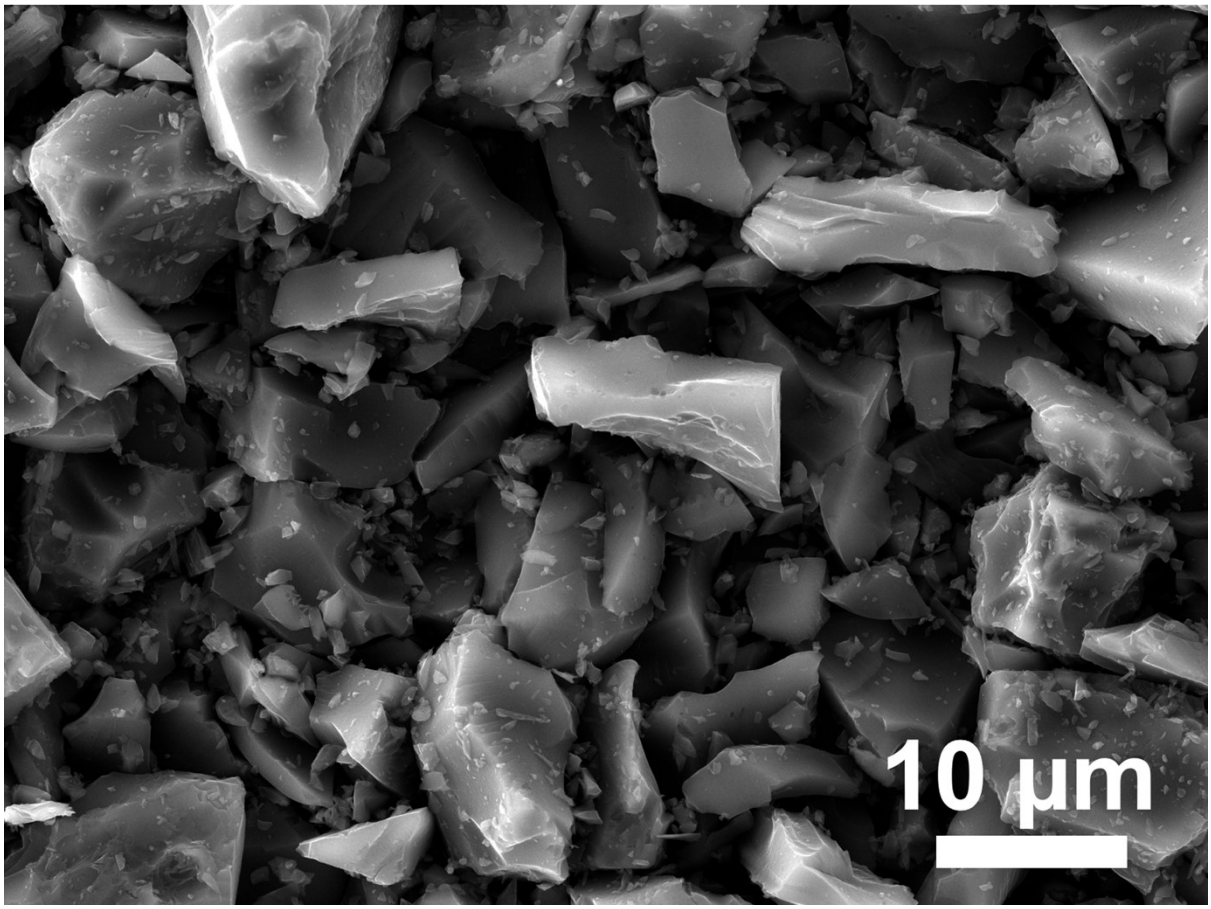

SI Figure S2: ***SEM micrograph of the activated carbon electrode.*** *Scanning electron micrograph of the MSP-20X activated carbon electrode containing 5 wt.% PTFE binder, recorded with a TESCAN CLARA field-free UHR scanning electron microscope (SEM) using an accelerating voltage of 10 keV and an Everhart-Thornley detector for secondary electron contrast.*

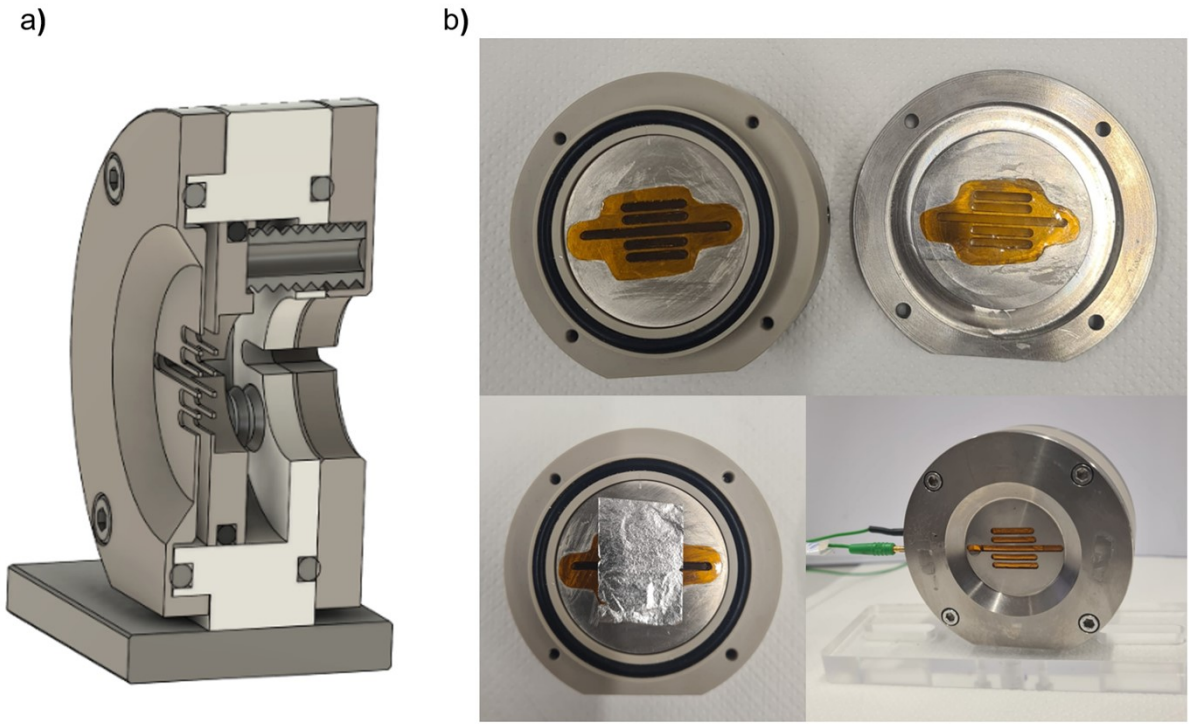

SI Figure S3: ***Operando X-ray cell design and assembly.*** *a) Cross-sectional rendering of the operando cell, showing the spring-loaded electrode area. The body is made from PEEK, the electrode plates are made from titanium. There are three springs with a spring constant of 25 N/mm that were compressed by a maximum of 4 mm in the assembled state, which results in a maximum combined spring force of* $3 * 4 * 25 = 300$ *N. With a circular cell design and a plate diameter of 40 mm, this resulted in an overall pressure of* $300/(40^2 * \pi/4) = 0.24$ *N/mm2 = 2.4 bar. b) Photographs of the individual cell components and the assembled device: the Kapton windows glued to the electrode plates, the Pt current collector foil, and the fully assembled cell. The Pt current collector foil shown in panel b) is for illustration only; during the operando experiments, a foil covering the full electrode plate was used.*

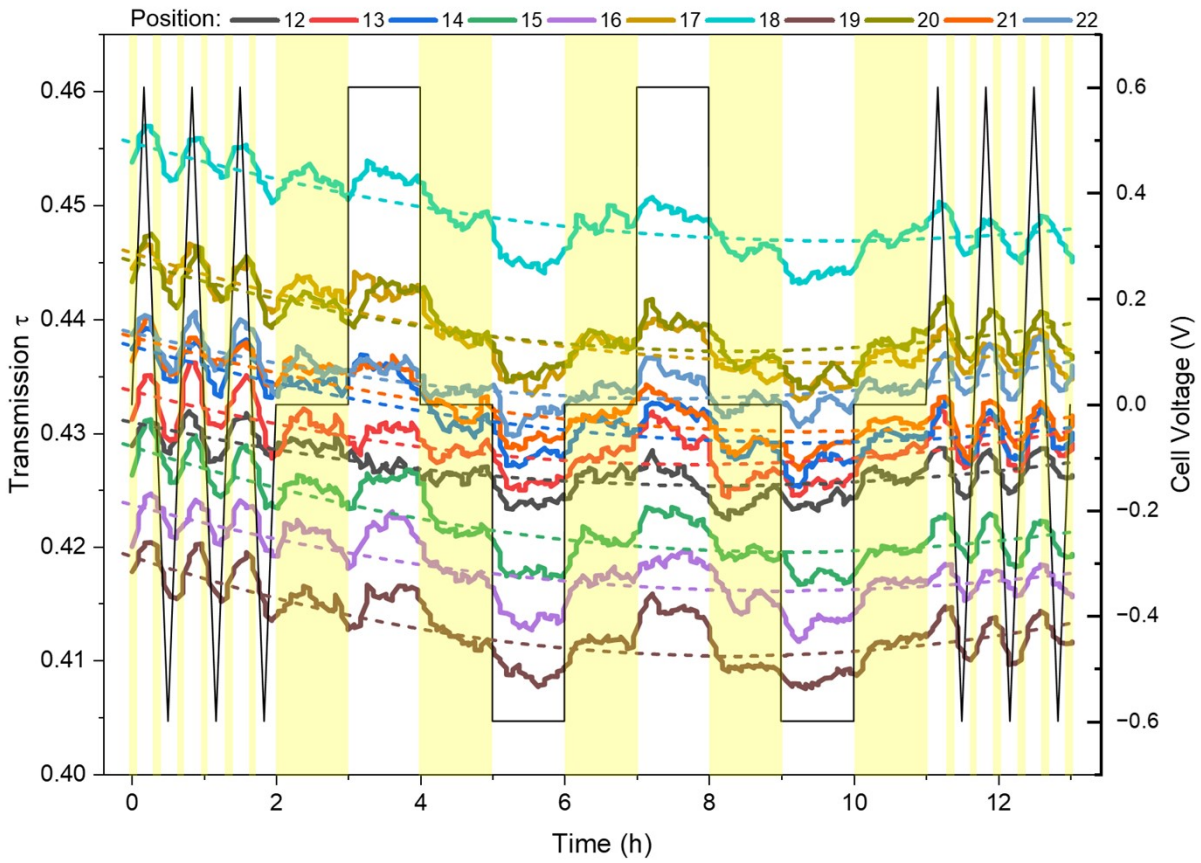

SI Figure S4: ***Determination of baseline transmission functions****. The solid lines show the raw transmission signals for selected positions on the working electrode according to the colour code on top of the panel (see SI Figure S5 a) in the SI or Figure 1 b) in the main manuscript). The dotted lines represent the corresponding second-degree polynomial baseline functions used for normalisation. These baselines were obtained by fitting the transmission values recorded during periods of 0 V cell voltage (highlighted in pale yellow). A slow drift towards lower absolute transmission values is observed over time, which has previously been reported and has been tentatively attributed to a gradual increase in the ion concentration within the electrode[1]. In some datasets, a very slight upturn at late times is visible, which is not interpreted as a physical effect and may arise from instrumental drift or limited sensitivity of the baseline correction for the final 0 V cell voltage nodes of the fit.*

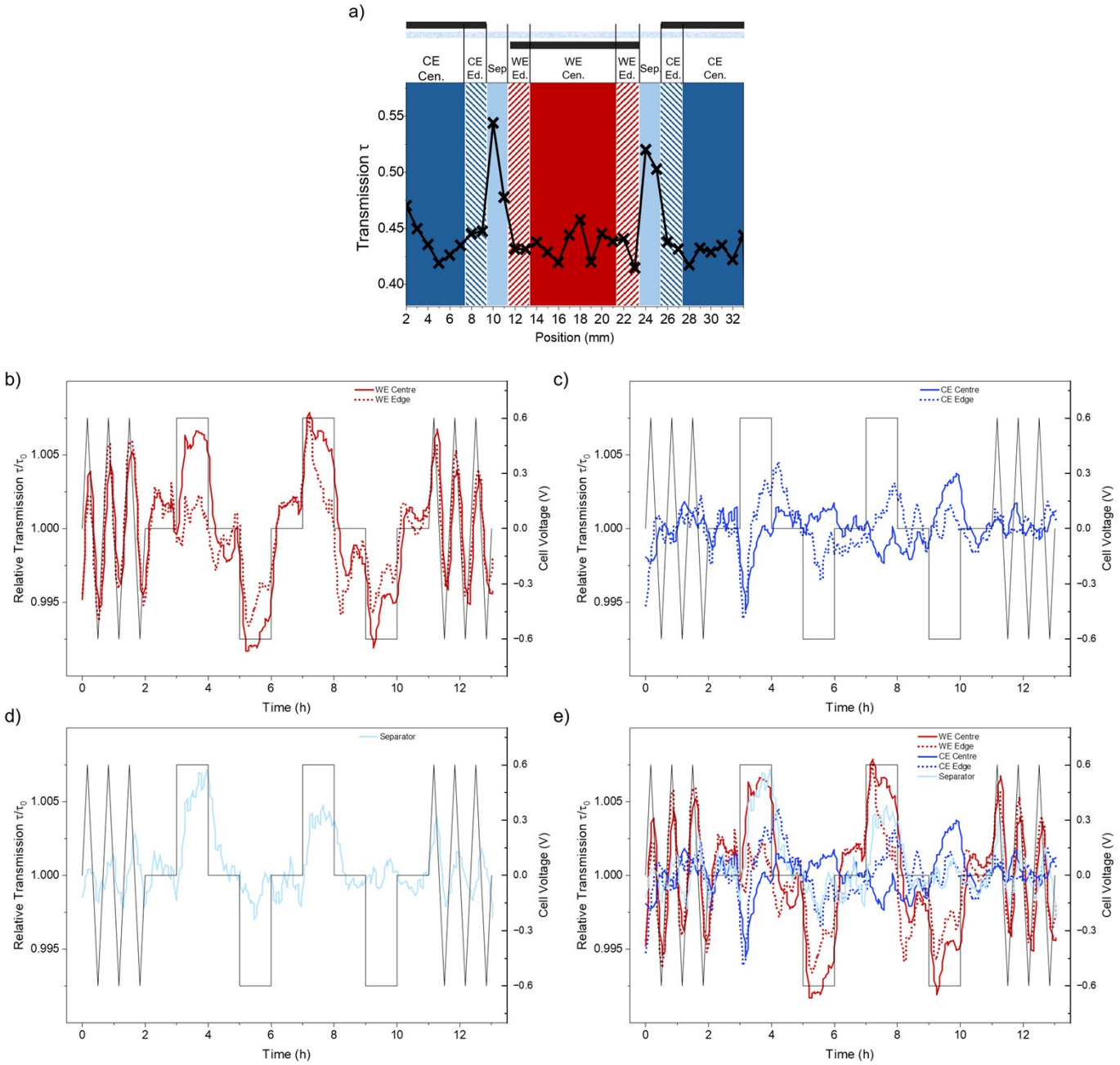

SI Figure S5: ***Transmission signals of different parts of the electrode stack.*** *a) XRT scan across the full electrode stack indicating the positions corresponding to the individual components as well as centre and edge regions. b) Relative transmission signal (τ/τ_0) of the working electrode (WE) averaged over centre and edge regions. c) Relative transmission signal of the counter electrode (CE) averaged over centre and edge regions. d) Relative transmission signal of the separator region. e) Overlay of all signals from b)-d) for comparison.*

Supplementary Note 1:

Operando X-ray fluorescence (XRF) measurements for a different electrode geometry were performed at the European Synchrotron Radiation Facility (ESRF) in Grenoble, France, on beamline ID22 under proposal SC5511. The operando cell, electrode material, and electrolyte were identical to those described in the main manuscript for the laterally arranged electrodes. A symmetric, stacked electrode configuration (see inset in SI, Figure S6 a)) was employed, using 14 mm diameter electrodes with 2 mm holes in either of the two electrodes to minimise deviations from a standard symmetric geometry while ensuring only one electrode is irradiated at a time. The X-ray experiments were carried out using a photon energy of 60 keV, a beam size of 1 × 1 mm^2, and an exposure time of 5 s. Accounting for stage movement between positions, each measurement was repeated approximately every 140 s. The applied potential sequence consisted of two-hour constant cell voltage holds at 0 V → +0.6 V → 0 V → −0.6 V → 0 V.

The integrated intensity of the XRF-lines from Rb and Br is directly proportional to the concentration of the respective element in the volume illuminated by the X-ray beam. Three distinct fluorescence peaks at 11.89 keV, 13.37 keV, and 14.96 keV are observed in the XRF signal (SI Figure S6 a)). The peak at 11.89 keV corresponds to Br Kα (Kα_1 an Br Kα_2 not being resolved). No neighbouring Rb emission lines are expected in this energy range. Therefore, this peak is referred to as the “Br peak”. The assignment of the peak at 13.37 keV is less clear, as it may arise from Rb Kα or Br Kβ. Since this peak does not exclusively correspond to either ion species, it was not further evaluated. The peak at 14.96 keV closely aligns with Rb Kβ_1 and is thus designated as the “Rb peak” with no near Br peaks nearby. The presence of well-separated, non-overlapping peaks enables a direct, ion-specific evaluation of the XRF spectrum. SI Figure S6 b) shows that at positive cell voltage, the Br^- concentration increases, while the Rb^+ concentration decreases. The opposite trend is observed at negative cell voltages, consistent with the expected concentration changes based on the polarity of the applied voltage. Since the magnitude of the concentration change for each ion species is comparable at both positive and negative polarisation (but with opposite sign), this indicates ion exchange with no preferred mobilization of either ion species. Interestingly also here, however, is the seemingly slower diffusion of Br^- (dashed line) as compared to Rb^+ (dotted line) during charging and discharging.

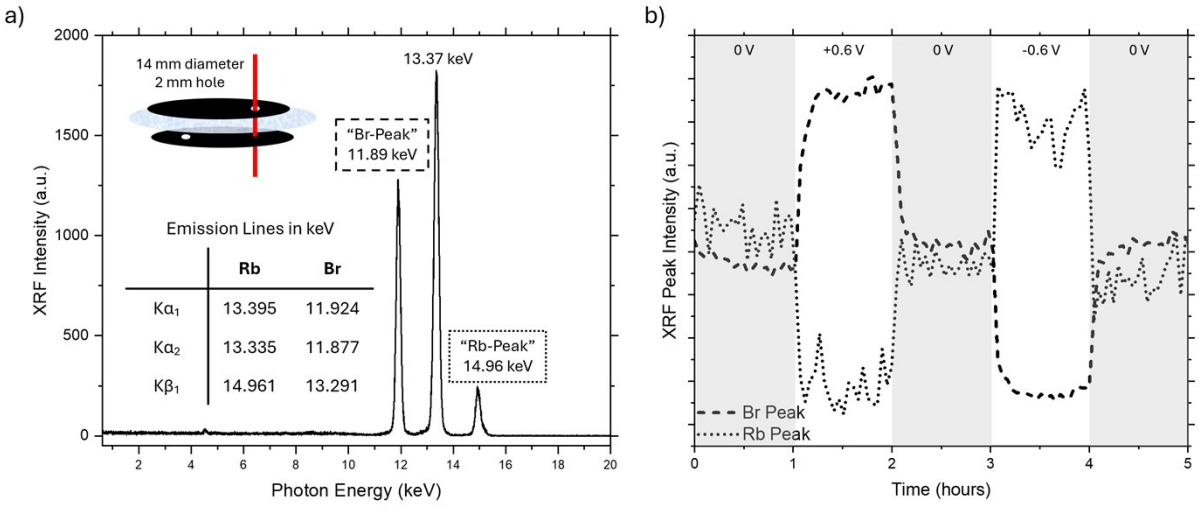

*Figure S6: **X-ray Fluorescence (XRF) spectrum of a symmetric electrode configuration.** a) Schematic illustration of the electrodes and the corresponding XRF spectrum at 0 V. The inset shows principal K-shell emission lines for Rb and Br, with data from Ref.[2]. b) Temporal evolution of the “Br peak” and “Rb peak” intensities during constant cell voltage holds at 0 V, +0.6 V, 0 V, −0.6 V, and 0 V, each held for 2 hours.*

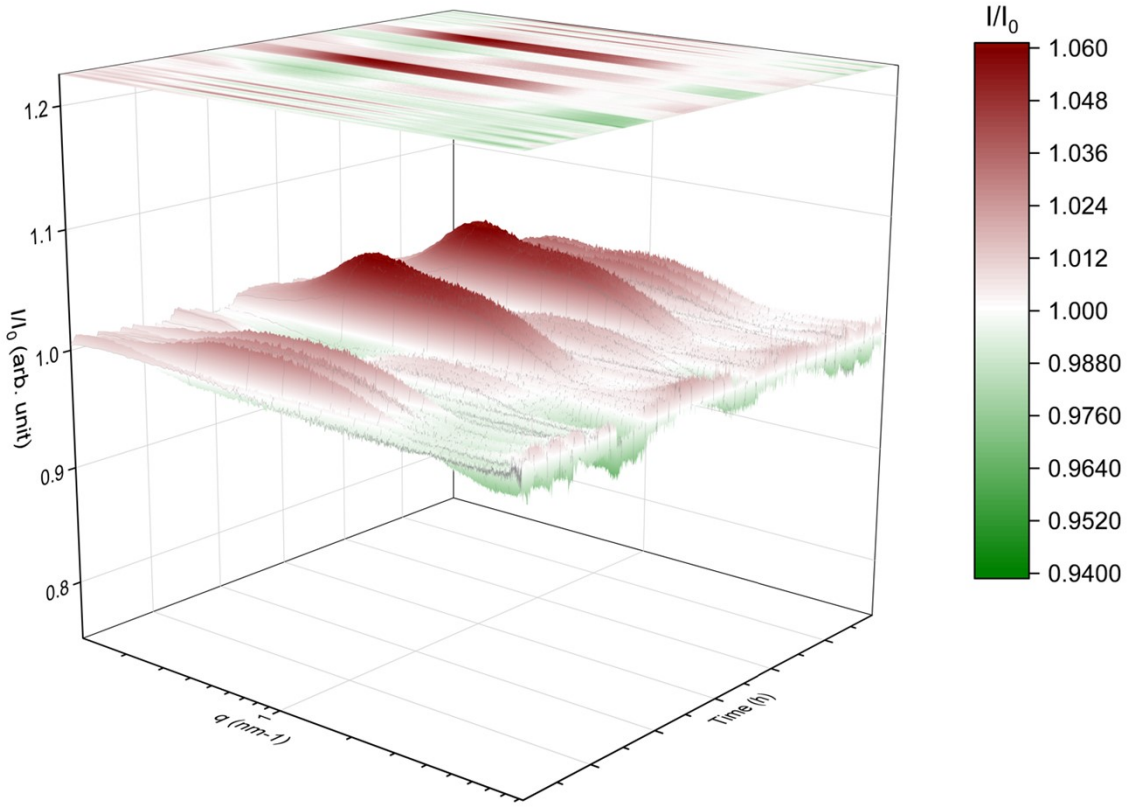

SI Figure S7: ***Three-dimensional representation of the operando SAXS data for a single scan position.*** *3D plot of the normalised scattering intensity I/I_0 as a function of scattering vector q and time for one representative scan position during the operando experiment. Red: increased contrast; green: reduced contrast, compared to the average contrast at 0 V applied cell voltage. Such datasets were collected for all scan positions. The top-view projection illustrates how the 2D heatmaps shown in the main text were obtained from the full time-resolved 3D dataset.*

SI References

1 M. Seyffertitz, S. Stock, M. V. Rauscher, C. Prehal, S. Haas, L. Porcar and O. Paris, *Faraday Discuss*, 2024, 249, 363–380.

2 Lawrence Berkeley National Laboratory: Energies of X-ray Emission Lines, https://xdb.lbl.gov/Section1/Table_1-2.pdf, (accessed 1 March 2025).